Idle Speed Control: An old problem in a new engine design[1]

Yan Wang[‡], Anna Stefanopoulou[‡], Mike Levin[+]
[‡] Mechanical and Environmental Engr. Dept., UC Santa Barbara
[+] Scientific Research Laboratory, Ford Motor Company

Abstract

The idle speed control problem of a spark ignited engine equipped with camless valvetrain is considered. The camless valvetrain allows control of the individual cylinder valves and can be used to achieve unthrottled operation, and consequently, improve dramatically fuel economy. We formulate the speed control problem for this engine and show that it exhibits unstable open loop behavior with a significant delay in the feedback loop. The instability is intrinsic to the unthrottled operation and specific to the camless actuation used to achieve the unthrottled operation. The delay is caused by the discrete combustion process and the actuator/sensor interface. We demonstrate the inherent system limitations associated with the unstable dynamics and the delay and provide insight on the structural (plant) changes that can alleviate these limitations. Finally, a stabilizing controller is designed and tested on a crankangle-based simulation model.

1 Introduction

In this paper we study the idle speed control problem of an unthrottled spark ignition engine equipped with an electro-hydraulic camless and springless valvetrain. In contrast to the majority of conventional automotive engines that operate with a valve motion fixed to the crankshaft rotation through the mechanical link of the camshaft, the camless valvetrain system allows fully controlled valve events. And, although the conventional system has proven to be convenient and safe, it compromises combustion stability, fuel economy, and maximum torque objectives. The camless valvetrain, on the other hand, allows the optimization of the exhaust and intake valve timing, motion, and activation for individual cylinder gas exchange control.

Various studies have shown that a camless valvetrain can alleviate many of engine design tradeoffs by supplying extra degrees of freedom to the overall powertrain system [1, 6, 9]. In particular, it has been shown that controlling the intake valve events can eliminate the need for throttled operation in the gasoline engines and thus obtain high fuel economy benefits [3, 8, 2]. In conventional gasoline engines the largest amount of throttling corresponds to the idle speed mode. It is, therefore, clear that unthrottled camless operation will result in significant fuel saving if applied to idle operation. Hence, one of the critical steps in obtaining the projected steady-state benefits of camless technology is the design of an idle speed controller for this innovative engine configuration.

To this end, we first analyze the open loop dynamics pertinent to the camless unthrottled operation. It is then demonstrated that the speed regulation problem in a camless engine is more challenging than the Idle Speed Control (ISC) problem for a conventional throttled operation. Specifically, the camless engine exhibits unbounded speed drop due to bounded (even, infinitesimally small) torque disturbance. The instability is intrinsic to the unthrottled operation and specific to the camless actuation used to achieve the unthrottled operation. It is, indeed, well known in the automotive community that "stable" unthrottled engine operation is difficult to achieve during low load, and in particular, during idle conditions [12, 14]. With this work we substantiate this observation and develop the necessary framework to analyze and control the process. Furthermore, we use system theoretic tools to obtain the limits of achievable performance. Our analysis and control design is based on a mean-value model, and the testing of the controller design is based on a crankangle simulation model developed in [2].

2 Camless Speed Dynamics

The objective of ISC is to maintain constant (and low) engine speed during application of loads. For a comprehensive review of ISC see [5]. In a ISC problem, the commonly chosen control variable is the throttle angle (or air bypass valve). Sometimes, the spark timing and the fuel ratio are also chosen, but in most cases, these actuators are reserved for other engine control functions. In the unthrottled camless engine we utilize the intake valve duration for cylinder air flow regulation instead of throttle or air by-pass valve. Wherever necessary in our camless ISC analysis we draw comparison with the air by-pass valve control of a conventional throttled engine.

One of the idle speed control design difficulties, common to all spark ignited engines, arises from the variable induction-to-power delay and the actuator authority which imposes a fundamental limitation to the closed loop bandwidth and restrict the disturbance rejection ability of the idle speed controller. Good fuel economy and emissions require low idle speed which aggravates the above difficulties because it results in longer delay, and therefore, it increases the limitations on the closed loop bandwidth. Moreover, low speed

[1] Research supported in part by the National Science Foundation under contract NSF ECS-97-33293; matching funds were provided by FORD MO. CO.

induces noise and combustion instability. To make things worse, the driver's perception of NVH characteristics is more acute during idle conditions making smooth idle speed operation a major customer concern.

A lumped parameter model can be used to describe the rotational dynamics that govern the crankshaft speed:

$$J\frac{dN}{dt} = T_{qe} - T_{qf} - T_{qd} \tag{1}$$

where T_{qe} is the engine generated torque, T_{qf} is the friction torque, and T_{qd} is the disturbance torque. The engine and friction torque are determined in [13] using experimental data for constant air-to-fuel ratio and spark timing, and zero exhaust gas recirculation:

$$T_{qf}(t) = F_{T_{qf}}(N(t)) \tag{2}$$
$$T_{qe}(t) = F_{T_{qe}}(m_{cyl}(t-\tau), N(t)). \tag{3}$$

In the engine torque equation (3), τ is the delay between the mass charge formation and the torque generation; we call it Induction-to-Power delay, **I-P delay**. The delay is triggered in crankangle-domain, and therefore, it is a function of the engine speed (N): $\tau = 2\Delta T$, where $\Delta T = \frac{120}{nN}$ is the fundamental engine event, and $n = 4$ for a 4-cylinder engine.

In the presence of a torque disturbance (T_{qd} in 1), the ISC task is to adjust the cylinder air charge (m_{cyl}) and generate the necessary engine torque (T_{qe}) to maintain constant engine speed (N). Thus, the ISC depends on the cylinder air charge regulation which is accomplished by directly controlling the intake valve duration, instead of indirectly controlling the intake manifold pressure. This difference is of central importance in the speed control problem because it results in unstable open loop dynamics. In comparison to the conventional throttled breathing dynamics the unthrottled camless breathing process lacks the stabilizing effects of the intake manifold filling dynamics. Reference to the absence of the self-regulating properties of the intake manifold dynamics can be found in the experimental study by Urata et al. in [14]. We confirm their observation with the following analysis of the breathing dynamics.

2.1 Self Regulation in Breathing

The electro-hydraulic actuator allows control of the lift and the timing (closing and opening) of the intake valve. Hence, the same value of air charge can be achieved by multiple combinations of valve lift, opening, and duration. Sensitivity analysis in [2] has shown that the valve duration is the most effective actuator in controlling air charge. We, thus, fix the valve opening and lift to values that satisfy minimum pumping losses and maximum turbulence requirements, and we only consider the valve duration for control purposes.

By assuming a uniform in time cylinder air flow we calculate the mean-value engine pumping rate ($F^{cml}_{m_{cyl}}$) for the camless engine which is a function of the valve duration (IVD) and engine speed (N). In contrast to the camless unthrottled operation, the conventional throttled engine pumping rate ($F^{cnv}_{m_{cyl}}$) is a function of the intake manifold pressure (p_m) and the engine speed (N) as shown in the equation below:

$$\dot{m}_{cyl} = F^{cml}_{m_{cyl}}(N, IVD) \tag{4}$$
$$\dot{m}_{cyl} = F^{cnv}_{m_{cyl}}(N, p_m). \tag{5}$$

The nonlinear static functions $F^{cml}_{m_{cyl}}$ and $F^{cnv}_{m_{cyl}}$ have been identified in [2] and are not included here due to space limitations. Figure 1 shows the block diagrams of the camless unthrottled and the conventional throttled engine dynamics. The rotational dynamics, friction, and torque generation blocks are the same for the two engines. Moreover, the engine speed has the same effects in both (throttled and unthrottled) engine pumping rates. In particular, a speed drop due to a torque disturbance will cause cylinder air flow to decrease, which if not corrected, can pontentially cause a large transient. This is an internal feedback that exists in both throttled and unthrottled engines. In the case of

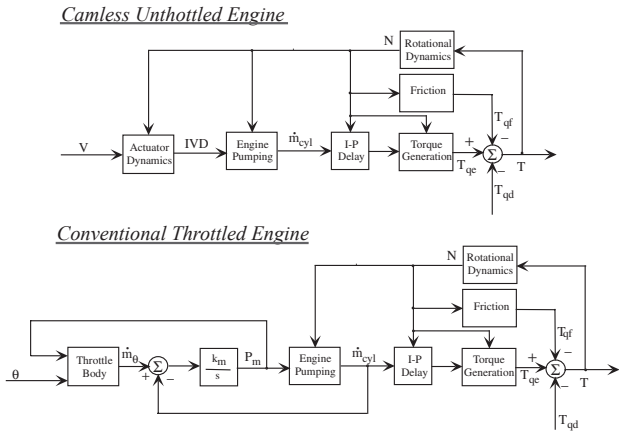

Figure 1: Nonlinear model of the camless unthrottled and the conventional throttled operation.

the conventional throttled engine the dependency of pumping rate on manifold pressure (p_m) creates another feedback loop that rejects the effect of engine speed on cylinder air flow. This is achieved through (i) the intake manifold filling dynamics that are modeled with the integrator shown in Figure 1, and (ii) the specific topology of the engine speed variations in the feedback loop. Thus the self-regulating effects of the manifold filling dynamics reject the cylinder air flow variations before they get to propagate to the rotational dynamics causing speed instability.

Unfortunately this is not the case with the camless unthrottled operation. Unthrottled conditions result in constant intake manifold pressure (approximately equal to the atmospheric pressure) which eliminates the manifold filling dynamics . By loosing the pumping rate dependency on the manifold pressure we loose the self regulating ability of the intake manifold filling dynamics. Moreover the actuator is a function of speed which amplifies the speed to cylinder flow dependency.

2.2 Camless Actuation

The majority of electro-hydraulic or eletro-mechanical actuators used for camless valvetrain development are trigerred in the time domain which has important implications in the engine dynamics. In this work the camless actuation is achieved with an electro-hydraulic system introduced in [9] and modeled in [7]. The valve motion is controlled by a sequence of pulses generated by electronics circuits. Figure 2 shows the Intake Valve Profile (IVP) and its associated two pulses that trigger the opening, lift, and closing of the valve. The valve opening and closing are triggered by t_{open} and t_{close}, respectively. From t_{open} to $t_{open} + \Delta t$, the valve moves with constant acceleration, hence, Δt controls the peak lift of the valve. By simplifying the trapezoidal valve profile with an ideal rectangular it is clear that the intake valve duration is controlled by the difference in the pulse timing $v = t_{close} - t_{open}$. As we mentioned earlier, the cylinder air charge is more sensitive to the duration rather than the lift, especially, if the lift is above 3 mm. For this reason, we choose the Intake Valve Duration (IVD) as the effective actuator of the breathing process.

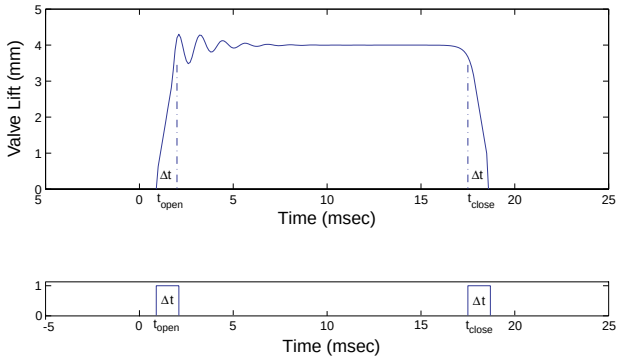

Figure 2: Intake valve profile generated by a pulse sequence.

From Figure 2, it is obvious that the degrees of IVD are controlled in the time domain by the time elapsed between the two pulses ($v = t_{close} - t_{open}$), which we call with slight abuse of notation as the **Pulsewidth**. The pulsewidth (v) is scheduled in time domain, therefore, the exact value of (crankangle) degrees of IVD is a function of engine speed:

$$\begin{aligned} IVD(t) &= F_{IVD}((N(t), v(t-\tau_\alpha)) \\ &= 0.006 N(t) v(t-\tau_\alpha), \end{aligned} \quad (6)$$

where, τ_α is the combination of sensing and controller-host computer communication delay. The initial experimental hardware indicates that a worst-case scenario results in a delay equal to one cycle, i.e., $\tau_\alpha = 4\Delta T$ (see Section 2 for the definition of ΔT).

One can see that, if an increase in load causes a drop of 200 rpm in nominal engine speed, and there is no adjustment to the valvetrain pulse-width (open-loop system), then the demanded valve duration reduces by 16.8 degrees. For illustration we add Figure 3. The solid line shows the camless intake valve profile (IVP) for a 14 msec pulse-width (input to the actuator) at 800 rpm, whereas the dashed line shows the valve profile that is generated by the same pulse-width (14 msec) at 600 rpm. The decrease in intake valve duration results in a decrease in cylinder air flow, and consequently, a further decrease in engine speed. This relationship constitutes the second positive feedback loop inherent to the speed dynamics of a camless engine.

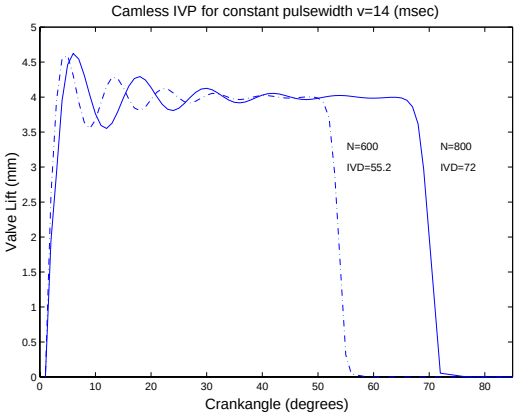

Figure 3: Intake valve profile for constant input pulsewidth ($v = 14$ ms) for 800 and 600 rpm.

3 Linearization

In the sections above it has been demonstrated that the camless engine is an unstable and highly nonlinear system with considerably large delays associated with the sensing/actuating interface and the discrete nature of the torque generation. The existence of unstable open loop dynamics and delays in the feedback loop imposes well known constraints in the closed loop performance depending on their relative effect.

Without downplaying the issues associated with the complex nonlinearities of the system, we are focusing on small-signal analysis and employ techniques pertinent to LTI systems. Linearization at a nominal point that corresponds to idle operation shows that the open loop dynamics of the unthrottled camless engine have a RHP pole and a significant delay. To assess potential difficulties in the feedback controller design, we first model the time delay as a non-minimum phase (NMP) zero using 1^{st} order *Padé* approximation, and then, apply well known results on fundamental limitations for finite dimensional systems. Analysis of the pole and zero relative location and sensitivity can be used to assess the inherent system limitations for a wide class of causal, stable, and linear stabilizing controllers.

Figure 4 shows the block diagram of the linearized model that is obtained by the linearization of nonlinear equations (2)-(6):

$$\Delta T_{qf} = k_N \Delta N \quad (7)$$

$$\Delta T_{qe} = k_{q1} e^{-\tau s} \Delta m_{cyl} + k_{q2} \Delta N \quad (8)$$

$$\Delta m_{cyl} = k_{m1}\Delta\dot{m}_{cyl} - k_{m2}\Delta N \quad (9)$$

$$\Delta IVD = k_{v1}e^{-\tau_\alpha s}\Delta v + k_{v2}\Delta N \quad (10)$$

Here we should note that all the coefficients "k_{xx}" are positive and are functions of the nominal operating inputs N_0 and v_0. Using the linear, lumped parameter rotational dynamics in (1) and 1^{st} order *Padé* approximation for the delays we obtain the following open loop transfer function:

$$\Delta N = \frac{-k_{v1}k_{u1}k_{m1}k_{q1}(s-z_u)(s+z_s)}{J(s+p_\tau)(s-p_s)(s-p_u)}\Delta v - \frac{s+z_s}{J(s-p_s)(s-p_u)}\Delta T_{qd}, \quad (11)$$

where, $p_\tau = -\frac{2}{\tau+\tau_\alpha}$ is a stable pole due to the delay approximation, and p_s, p_u are the remaining stable (LHP) and unstable (RHP) poles of the characteristic equation. In the above equation, we denote as $z_s = -\frac{2}{\tau_\alpha}$ and $z_u = \frac{2}{\tau+\tau_\alpha}$ the minimum- and nonminimum-phase zeros of the transfer function.

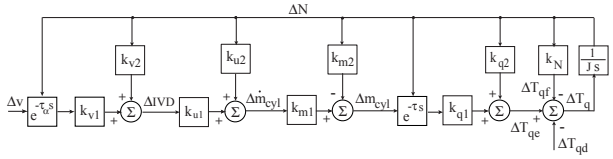

Figure 4: Linearized model of the camless unthrottled engine

Linearization of the camless engine model at nominal engine speed $N_0 = 800$ rpm, and valve pulsewidth $v_0 = 13.9$ ms that corresponds to typical idle speed conditions results in a RHP pole $p_u = 0.3$ and a NMP zero $z_u = 8.9$. Their relative location ($z_u > 4p_u$) is not restrictive if one adheres to the "rule of thumb" that the open loop crossover frequency (ω_c) should be $2p_u \le \omega_c \le z_u/2$ (see [4, 10, 11]). An investigation of the pole-zero location for a range of pulsewidths and speeds shows that the RHP pole and the NMP phase zero stay one decade apart which does not pose a great obstacle in the controller design for the specific experimental vehicle we considered. Moreover, the system becomes stable at nominal pulsewidth $v_0 = 13.9$ ms and nominal speed N_0 =1700 rpm.

On the other hand, a brief calculation of the pole-zero location for a vehicle with smaller inertia indicates a difficult feedback problem with $z_u \approx 3.3p_u$. Similar difficulties were found for operation under heavy load. Eventhough, these "difficult" cases are application specific, they indicate the need for a comprehensive study of the relative pole and delay value in order to assess the system feasibility.

4 Feedback Limitations

We consider a unity SISO feedback system with a linear, causal and stable controller $C(s)$ as shown in Figure 5, where ΔN is the engine speed variation, Δr is the desired engine speed variation, Δv is the pulsewidth variation, ΔT_{qd} is the torque load variation. According to the transfer function (11), we get:

$$G_u(s) = k_{v1}k_{u1}k_{m1}k_{q1}\frac{s-z_u}{s-p_\tau} \quad (12)$$

$$G_d(s) = \frac{-(s-z_s)}{J(s-p_s)(s-p_u)}. \quad (13)$$

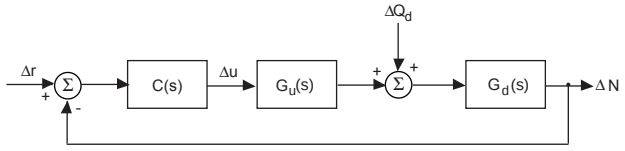

Figure 5: Unity feedback control system for the camless unthrottled engine.

Let $L(s) = C(s)G_u(s)G_d(s)$ be the open loop transfer function, $S(s) = 1/(1+L(s))$ the sensitivity function, and $T(s) = L(s)/(1+L(s))$ the complementary sensitivity function. The idle speed control objectives can be summarized as good disturbance rejection with small control effort, thus, the transfer functions of interest are:

$$\begin{aligned}\Delta N(s) &= T(s)\Delta r(s) + S(s)G_d(s)\Delta T_{qd}(s)\\ \Delta v(s) &= C(s)S(s)\Delta r(s) - C(s)S(s)G_d(s)\Delta T_{qd}(s).\end{aligned} \quad (14)$$

For the ISC problem, we set $\Delta r = 0$, and (14) can be simplified:

$$\Delta N(s) = S(s)G_d(s)\Delta T_{qd}(s) \quad (15)$$

$$\Delta u(s) = -C(s)S(s)G_d(s)\Delta T_{qd}(s). \quad (16)$$

The well known result $2p_u \le \omega_c \le z_u/2$ used above, indicates that a stable controller exists, but, it does not guarantee that the achieved closed loop performance and robustness will be acceptable for the stringent idle speed control requirements. Further investigation is required using realistic bounds on sensitivity that reflect desired specifications on the disturbance rejection of the ISC. Examples of such bounds can be found in [15], or one can interpret time-domain specifications found in [5]. A typical test for the ISC problem consists of a 15 Nm (unmeasured) torque disturbance and a minimum desired disturbance rejection bandwidth of 1.3 rad/sec. The minimum requirements for low frequency disturbance rejection introduces an upper bound on the sensitivity function. This bound is modeled by $w_p(s) = (\frac{s}{M_S} + {\omega_B}^*)/s$ where the minimum desired bandwidth is ${\omega_B}^*$ =1.3 rad/sec (${\omega_B}^*$ is the frequency where the straight-line approximation of w_p is equal to 1) and M_S is the sensitivity peak. Using the interpolation constraint $S(z_u) = 1$ that the NMP zero introduces, we conclude that

$$|w_p(z)| = |w_p(z)S(z)| \le \|w_pS\|_\infty \le 1. \quad (17)$$

The last inequality reflects the performance specification $\|w_pS\|_\infty < 1$. Solving (17) for M_S suggests that the closed

loop system might have unacceptable robustness properties in intermediate frequencies, i.e., $M_S = 3.8$.

Note here that analysis of the feedback limitations associated with the unstable pole ($T(p_u) = 1$) does not point to any additional difficulties, other than the need for a stabilizing controller ($T(p_u) = 1 \Rightarrow \|T\|_\infty \geq 1$ which requires $C(s) \neq 0$). Similarly, the integral constraints associated with the existence of a RHP pole and the NMP zero do not pose any additional difficulties. The same conclusion holds even if we consider the more restrictive phase limitations of the delay instead of optimistically approximating with a NMP zero. These simple calculations lead us to the conclusion that the open loop instability does not impose a significant limitation in the feedback design. On the other hand, the system instability requires a detailed analysis and formal ways of testing software interrupts and priorities among tasks. Although non-trivial, these implementation issues have been successfully addressed in production of diesel fuel governors and injection systems.

From the analysis above it is clear that the long (one cycle) delay due to controller/hardware interface limit the closed loop performance. For comparison consider the conventional engine at idle conditions. The location of RHP-zero is at $z_{conv} = 2\frac{1}{\Delta T} \approx 26.7$. Obviously the small delay in the conventional feedback allows $\omega_c \leq 13.3$, which implies faster disturbance rejection than what is currently feasible for the camless operation ($0.6 \leq \omega_c \leq 4.4$). Advances in real time computing and controller hardware are expected to eliminate this delay in the near future making camless technology a potential candidate for the new generation of highly efficient vehicles.

4.1 Simulation Results

A PI controller is designed for the camless ISC problem. A 15 Nm step torque disturbance is used to test the closed loop performance because it is considered a typical large load from the air-conditioning system. The dashed line in Figure 6 shows the closed loop speed response of the mean-value nonlinear engine-vehicle model. The solid line in the same figure shows the closed loop performance when the PI controller is implemented in a crankangle high-order simulation model. The maximum speed deviation for the mean-value model is 12 rpm, and the settling time is less than 2 sec. The closed loop simulation in the crankangle-domain shows 20 rpm deviation from the nominal and no significant degradation of the settling time.

5 Conclusions

In this paper, we formulated the idle speed control problem for a SI engine equipped with a camless electro-hydraulic valvetrain. We showed that unthrottled camless operation results in unstable open loop dynamics. We demonstrated using linear theoretic techniques that the unstable pole and the controller/hardware delay impose limitation in the achievable disturbance rejection performance of the closed loop system.

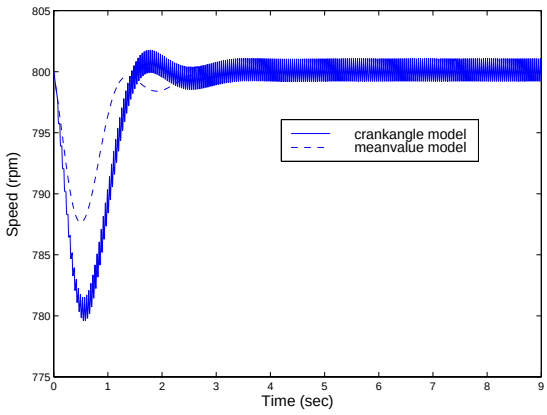

Figure 6: Step disturbance response for the closed loop mean-value and crankangle-based system.

References

[1] Ahmad T. and Theobald M. A., "A Survey of Variable Valve Actuation Technology," SAE 891674.

[2] Ashhab M. S., Stefanopoulou A. G., Cook J. A., and Levin M., "Camless Engine Control for Robust Unthrottled Operation," SAE 981031.

[3] Elrod A. C. and Nelson M. T., "Development of a Variable Valve Timing Engine to Eliminate the Pumping Losses Associated with Throttled Operation," SAE 860537.

[4] Freudenberg J. S., and Looze D. P., "Right Half Plane Poles and Zeros and Design Tradeoffs in Feedback Systems," IEEE TAC, Vol. AC-30, No. 6, pp. 555-556, June 1985.

[5] Hrovat D., and Sun J., "Models and Control Methodologies for IC Engine Idle Speed Control Design," Control Eng. Practice, Vol. 5, No 8, pp. 1093-1100, 1997.

[6] Gray C., "A Review of Variable Engine Valve Timing," SAE 880386.

[7] Kim D., Anderson M, Tsao T.-C., and Levin M., "A Dynamic Model of a Springless Electrohydraulic Camless Valvetrain System," SAE Paper, No. 970248.

[8] Miller R. H. et al., "Unthrottled Camless Valvetrain Strategy for Spark-Ignited Engines," Proc. 19th ASME Con., ICE-Vol. 29-1, pp.81-94, 1997.

[9] Schechter M. M. and Levin M. B., "Camless Engine," SAE 960581.

[10] Seron M. M., Braslavsky J. H., and Goodwin G. C., *Fundamental Limitations in Filtering and Control,* Springer-Verlag, 1997.

[11] Skogestad S., Postlethwaite I., *Multivariable feedback control: Analysis and Design*, J. Wiley & Sons, 1996.

[12] Sono H. and Umiyama H., "A Study of Combustion Stability of Non-Throttling SI Engine with Early Intake Valve Closing Mechanism," SAE 945009.

[13] Stefanopoulou A. et al., "Air-Fuel Ratio and Torque Control uing Secondary Throttle" Proc. 33rd IEEE CDC, pp. 2748-2753, 1994.

[14] Urata Y., Umiyama H., Shimizu K., Fujiyoshi Y., Sono H., and Fukuo K., "A Study of Vehicle Equipped with Non-Throttling SI Engine with Early Intake Valve Closing," SAE 930820.

[15] Williams S. J., Hrovat D., Davey C., Maclay D., Crevel J. W., Chen L. F., "Idle Speed Control Design Using an H_∞ Approach," Proc. ACC, pp.1950-1956, 1989.